Robotica (2002) volume 20, pp. 195–201. © 2002 Cambridge University Press
DOI: 10.1017/S0263574701003666 Printed in the United Kingdom

An inverse position analysis of five-bar planar parallel manipulators

Gürsel Alici

Gaziantep University, Faculty of Engineering, Department of Mechanical Engineering, TR-27310 Gaziantep (Turkey)
E-mail: gursel@gantep.edu.tr

(Received in Final Form: June 29, 2001)

SUMMARY

In this paper, we present a simple method to obtain joint inputs needed to attain any point in the reachable workspace of a class of five-bar planar parallel manipulators which are based on five rigid links and five single degree of freedom joints – revolute and prismatic joints. Depending on the topology of the manipulators, two mathematical expressions describing the path traced by the tip of two links connected to each other are obtained and solved simultaneously in order to determine the intersection points of the two paths which are the Cartesian coordinates of the connection points for the links. For the class of manipulators considered in this study, one of the links is the link activated by an actuator fixed to the ground. So, rotational and/or translational joint inputs can be determined from the Cartesian coordinates of the tip of the activated links. Sylvester's dialytic elimination method is employed to solve the equations. Such a methodology is easy to implement, computationally efficient and sound to compute all possible solutions. A numerical example is provided for each manipulator and the inverse position solutions are verified by substituting them into forward position equations. It is concluded that the proposed method is useful in trajectory planning and control of five-bar planar parallel manipulators in joint space.

KEYWORDS: Parallel manipulators; Inverse and forward kinematics; Elimination method; Trajectory planning

1. INTRODUCTION

Robot manipulators are anthropomorphic open loop mechanisms which usually have longer reach, larger workspace, and more dexterity than closed chain mechanisms. They also have some disadvantages; the cantilever-type of structure for open manipulators naturally has low stiffness and therefore has undesirable dynamic characteristics, especially at high speed and heavy loading conditions. Mainly due to these disadvantages; many robotics tasks based on the high level of accuracy in positioning of the manipulators' end point are not generally realisable by conventional serially connected robot manipulators. One approach to achieve the required level of accuracy is to consider alternative structural designs which are more rigid than serial manipulators. Parallel connection is an alternative type to the serial mechanisms where closed-loop kinematics chains are included into a robot manipulator so that the output can be produced by in parallel-actuated closed-loop kinematics chains,[1–3]. Parallel manipulators have the inherent advantages of better load carrying capability and more precise positioning of the payload – they are ideal for high-speed and high precision applications.

The inverse kinematics problem of a manipulator is the transformation of position and orientation of the end effector in Cartesian space into joint positions to be used by lower level joint controllers. The inverse kinematics problem is analytically complex and closed-form solutions do not always exist.[4–8] In this paper, we make use of Sylvester's dialytic elimination method, which is based on an algebraic formulation giving all common solutions and more insight into the solution than a purely numerical solution, such that the problem reduces to solve a single variable polynomial. The proposed method consists of: (i) obtaining two mathematical expressions which are nonlinear and describe the path traced by the tip of two links connected to each other, (ii) solving the nonlinear equations by employing Sylvester dialytic elimination method, finally (iii) verifying the inverse position solutions by substituting them into forward kinematics equations. Note that forward kinematics equations are not solved analytically or numerically to attain to the inverse position solution. This way of formulating the problem differs from work reported before. Application of an elimination method to solve kinematics problem is not new, it has been applied to serial manipulators,[9,10,12] and Stewart-platform based parallel manipulators before.[2,11]

A great deal of work has been conducted in the area of inverse kinematics of robot manipulators.[4–10,12,13] An in-depth discussion of kinematics analysis of robot manipulators and solution methods are found in reference [6]. The methods generally employed to solve an inverse kinematics problem are either *analytical* or *numerical*. An analytical solution is one that produces a particular mathematical expression or formula for each joint variable in terms of known end point position and orientation coordinates, whereas a numerical solution generally is to determine appropriate value of the joint variable as a result of an iterative computational procedure. In general, a numerical solution method is time consuming, sensitive to initial estimates and is rather slower than the corresponding analytical method and does not allow to obtain all possible solutions due to its iterative nature. On the other hand, a numerical method clearly has the advantage of being

https://doi.org/10.1017/S0263574701003666 Published online by Cambridge University Press

applicable to any robot manipulator. It is very important to find fast algorithms for the use of inverse kinematics in trajectory planning and position and force control, kinematics calibration and goal-oriented computer animation. The method presented is efficient computationally, easy to implement and numerically sound to obtain all possible solutions. It contributes to previously published work due to its simplicity and requiring very small computation time. Without imposing a significant computational burden on control computer, the proposed method is useful in trajectory planning and control of five-bar planar parallel manipulators in joint space.

2.1 Five-bar manipulators with revolute and prismatic joints

The number of the potential five-bar planar parallel manipulators made up of revolute and prismatic joints is thirty-two, which can be further reduced to six by considering some constraints described in reference [14]. They are RRRRR, RRRRP, PRRRP, RPRPR, RRRPR and RPRRP parallel manipulators, which are depicted in Figure 1. Their two joints are active and the rest are passive joints. If a five-bar mechanism consists of a single closed-loop and it has two active joints and three passive joints, such a mechanism is controllable and can be employed to position a point in a two dimensional space.[15] In reference [1], the singularity configurations of these parallel manipulators are given, but their inverse position analysis has not been described.

2.2 Forward kinematics equations

Consider the RRRRR parallel manipulator shown in Figure 2(a). For the provided joint inputs θ_1 and θ_2, and the specified link lengths $\mathbf{r}_0$, $\mathbf{r}_1$, $\mathbf{r}_2$, $\mathbf{r}_3$, $\mathbf{r}_4$, the analytical expressions for the coordinates of the output point **P** where the end effector is assembled to is obtained. The coordinates

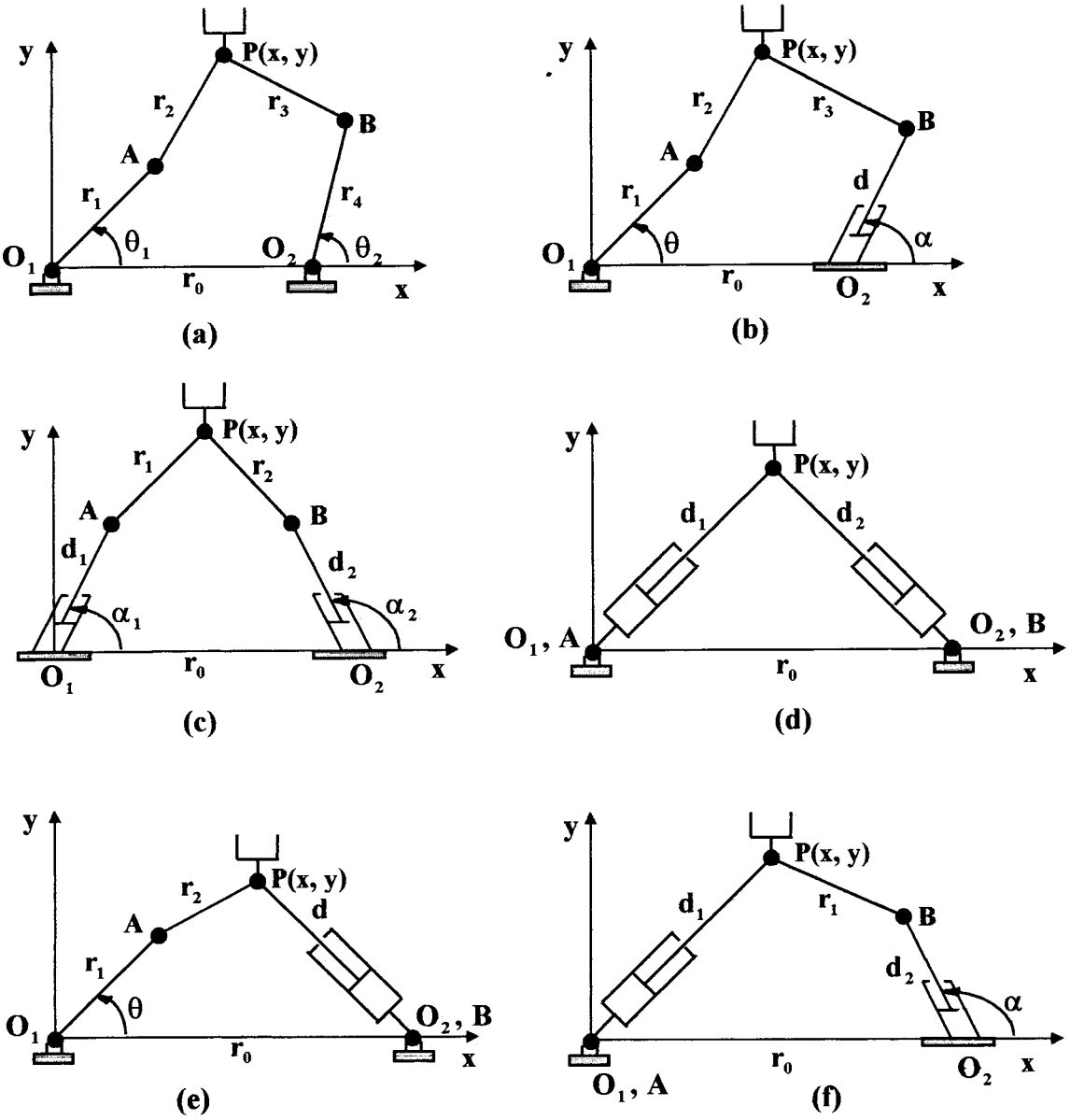


Fig. 1. A class of five-bar planar parallel manipulators.

https://doi.org/10.1017/S0263574701003666 Published online by Cambridge University Press

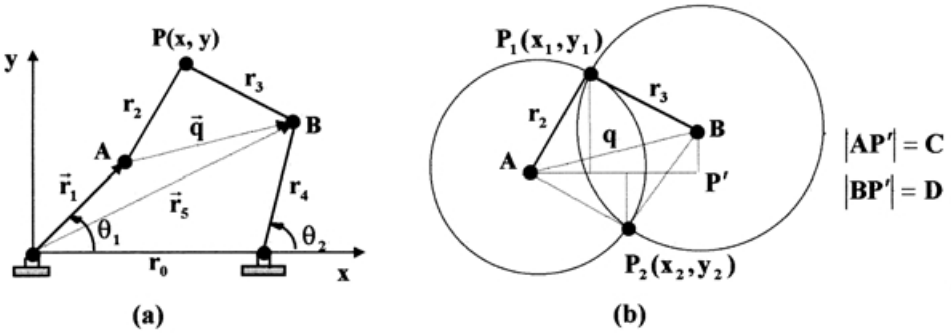


Fig. 2. Geometric representation of forward kinematics solutions.

of **A** and **B** which are the **x** and **y** components of the $\vec{\mathbf{r}}_1$ and $\vec{\mathbf{r}}_5$ vectors can be considered as the coordinates of the centers of two circles of radii $\mathbf{r}_2$ and $\mathbf{r}_3$. Note that the center of two circles are expressed as functions of the inputs provided by the actuators fixed to the ground. It is well-known that the intersection of the two circles gives a maximum of two solutions which are the possible locations of point **P**. Referring to Figure 2(b), the analytical expressions for these two solutions are obtained using the following algorithm;

$$\begin{aligned}\vec{\mathbf{r}}_1&=\mathbf{r}_1\cos\theta_1\,\vec{\mathbf{i}}+\mathbf{r}_1\sin\theta_1\vec{\mathbf{j}},\\ \vec{\mathbf{r}}_5&=(\mathbf{r}_0+\mathbf{r}_4\cos\theta_2)\,\vec{\mathbf{i}}+\mathbf{r}_4\sin\theta_2\vec{\mathbf{j}},\end{aligned}\tag{1}$$

$$\vec{\mathbf{q}}=\vec{\mathbf{r}}_5-\vec{\mathbf{r}}_1=\mathbf{C}\vec{\mathbf{i}}+\mathbf{D}\vec{\mathbf{j}}\tag{2}$$

$$\mathbf{C}=\mathbf{r}_{5x}-\mathbf{r}_{1x},\ \mathbf{D}=\mathbf{r}_{5y}-\mathbf{r}_{1y},\ \mathbf{q}=\sqrt{\mathbf{C}^2+\mathbf{D}^2},\tag{3}$$

$$\mathbf{Q}=\frac{\mathbf{r}_2^2+\mathbf{q}^2-\mathbf{r}_3^2}{2\mathbf{q}^2},\tag{4}$$

and the coordinates of $\mathbf{P}_1$ and $\mathbf{P}_2$ are;

$$\begin{aligned}\mathbf{x}_1&=\mathbf{x}_A+\mathbf{QC}-\mathbf{D}\sqrt{\frac{\mathbf{r}_2^2}{\mathbf{q}^2}-\mathbf{Q}^2},\\ \mathbf{y}_1&=\mathbf{y}_A+\mathbf{QD}+\mathbf{C}\sqrt{\frac{\mathbf{r}_2^2}{\mathbf{q}^2}-\mathbf{Q}^2},\\ \mathbf{x}_2&=\mathbf{x}_A+\mathbf{QC}+\mathbf{D}\sqrt{\frac{\mathbf{r}_2^2}{\mathbf{q}^2}-\mathbf{Q}^2},\\ \mathbf{y}_2&=\mathbf{y}_A+\mathbf{QD}-\mathbf{C}\sqrt{\frac{\mathbf{r}_2^2}{\mathbf{q}^2}-\mathbf{Q}^2}.\end{aligned}\tag{5, 6}$$

So, it is now possible to determine the position of the output point for given joint inputs. Depending on the link lengths, $(\mathbf{x}_1, \mathbf{y}_1)$ and $(\mathbf{x}_2, \mathbf{y}_2)$ can have real and imaginary values. If they are imaginary, some kinematics constraints are not satisfied; the mechanism can not be assembled in those configurations. Link lengths not causing this problem are used in numerical examples.

3. SOLVING AN INVERSE POSITION PROBLEM

Link lengths $\mathbf{r}_i$, the Cartesian coordinates $(\mathbf{x}_p, \mathbf{y}_p)$ of the manipulator tip point **P** and those of the actuators (active joints) are known. While each movable link in the mechanism connected to a revolute joint traces a circle whose radius is the link length, the link(s) connected to a prismatic joint traces a line. By making use of the intersection points of two circles or a circle with a line, we are able to determine joint inputs needed to reach the manipulator tip point specified in Cartesian coordinates. Referring to Figure 3(a), the equations of two circles of radii $\mathbf{r}_i$ and $\mathbf{r}_j$ centered at known points **C** and **D**, respectively, are;

$$\begin{aligned}(\mathbf{x}-\mathbf{x}_C)^2+(\mathbf{y}-\mathbf{y}_C)^2&=\mathbf{r}_i^2,\\ (\mathbf{x}-\mathbf{x}_D)^2+(\mathbf{y}-\mathbf{y}_D)^2&=\mathbf{r}_j^2\end{aligned}\tag{7}$$

The simultaneous solution of the equations in Eq. 7 will give two intersection points $(\mathbf{x}, \mathbf{y})_1$ and $(\mathbf{x}, \mathbf{y})_2$.

Referring to Figure 3(b), the equation of a circle of radius $\mathbf{r}_i$ centered at **E** and that of a line with a slope **m** and **y**-axis intercept **n**, respectively, are;

$$\begin{aligned}(\mathbf{x}-\mathbf{x}_E)^2+(\mathbf{y}-\mathbf{y}_E)^2&=\mathbf{r}_i^2,\\ \mathbf{y}&=\mathbf{mx}+\mathbf{n}\end{aligned}\tag{8}$$

The simultaneous solution of the equations in Eq. 8 will give two intersection points $(\mathbf{x}, \mathbf{y})_1$ and $(\mathbf{x}, \mathbf{y})_2$. Depending

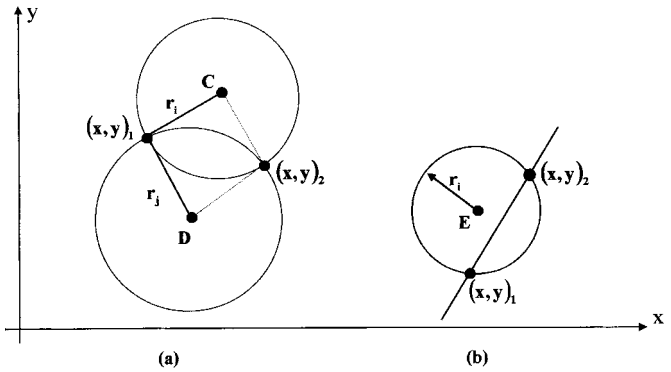


Fig. 3. Geometric representation of inverse position solutions for two links actuated (a) by two rotary joints, and (b) by one rotary – one translational joint.

https://doi.org/10.1017/S0263574701003666 Published online by Cambridge University Press

on the configuration of the manipulators considered in this paper, either Eq. 7 or Eq. 8 or both are employed to determine the tip of Cartesian coordinates of the activated links. Note that the expansion of Eq. 7 and Eq. 8 result in two nonlinear polynomial with two unknowns **x** and **y**. As presented in the next section, Sylvester elimination method is followed to solve the two equations simultaneously.

3.1 RRRRR manipulator

For $\mathbf{r}_i=\mathbf{r}_2$, $\mathbf{r}_j=\mathbf{r}_1$, $\mathbf{x}_C=\mathbf{x}_p$, $\mathbf{y}_C=\mathbf{y}_p$ and $\mathbf{x}_D=\mathbf{y}_D=\mathbf{0.0}$, the simultaneous solution of the equations in Eq. 7 give two intersection points $(\mathbf{x}_1, \mathbf{y}_1)_1$ and $(\mathbf{x}_1, \mathbf{y}_1)_2$ which are the Cartesian coordinates of the tip of the link $\mathbf{O}_1\mathbf{A}$ of the RRRRR manipulator shown in Figure 1(a). By using **atan2** function, the joint input θ_1 is determined. Similarly, for $\mathbf{r}_i=\mathbf{r}_3$, $\mathbf{r}_j=\mathbf{r}_4$, $\mathbf{x}_C=\mathbf{x}_p$, $\mathbf{y}_C=\mathbf{y}_p$, $\mathbf{x}_D=\mathbf{r}_0$ and $\mathbf{y}_D=\mathbf{0.0}$, the simultaneous solution of the equations in Eq. 7 will give two intersection points $(\mathbf{x}_2, \mathbf{y}_2)_1$ and $(\mathbf{x}_2, \mathbf{y}_2)_2$ which are the Cartesian coordinates of the tip of the link $\mathbf{O}_2\mathbf{B}$. By using **atan2** function, the joint input θ_2 is determined. Note that for a parallel RRRRR manipulator $\mathbf{r}_1=\mathbf{r}_4$ and $\mathbf{r}_2=\mathbf{r}_3$.

3.2 RRRRP Manipulator

For $\mathbf{r}_i=\mathbf{r}_2$, $\mathbf{r}_j=\mathbf{r}_1$, $\mathbf{x}_C=\mathbf{x}_p$, $\mathbf{y}_C=\mathbf{y}_p$ and $\mathbf{x}_D=\mathbf{y}_D=\mathbf{0.0}$, the simultaneous solution of the equations in Eq. 7 give two intersection points $(\mathbf{x}_1, \mathbf{y}_1)_1$ and $(\mathbf{x}_1, \mathbf{y}_1)_2$ which are the Cartesian coordinates of the tip of the link $\mathbf{O}_1\mathbf{A}$ of the RRRRP manipulator shown in Figure 1(b). By using **atan2** function, the joint input θ is determined. Similarly, for $\mathbf{r}_i=\mathbf{r}_3$, $\mathbf{x}_E=\mathbf{x}_p$, $\mathbf{y}_E=\mathbf{y}_p$, $\mathbf{m}=\mathbf{tan}\ \alpha$ and $\mathbf{n}=-\mathbf{r}_0\ \mathbf{tan}\ \alpha$, the simultaneous solution of the equations in Eq. 8 will give two intersection points $(\mathbf{x}_2, \mathbf{y}_2)_1$ and $(\mathbf{x}_2, \mathbf{y}_2)_2$ which are the Cartesian coordinates of the tip of the link $\mathbf{O}_2\mathbf{B}$. The corresponding actuator input **d** is calculated from the vectorial equation

$$\vec{d}=\overrightarrow{\mathbf{O}_1\mathbf{B}}-\overrightarrow{\mathbf{O}_1\mathbf{O}}_2 \Rightarrow \mathbf{d}=\sqrt{(\mathbf{x}_2-\mathbf{r}_0)^2+\mathbf{y}_2^2} \tag{9}$$

3.3 PRRRP manipulator

For $\mathbf{r}_i=\mathbf{r}_1$, $\mathbf{x}_E=\mathbf{x}_p$, $\mathbf{y}_E=\mathbf{y}_p$, $\mathbf{m}=\mathbf{tan}\ \alpha_1$ and $\mathbf{n}=\mathbf{0.0}$, the simultaneous solution of the equations in Eq. 8 give two intersection points $(\mathbf{x}_1, \mathbf{y}_1)_1$ and $(\mathbf{x}_1, \mathbf{y}_1)_2$ which are the Cartesian coordinates of the tip of the link $\mathbf{O}_1$A of the RRRRP manipulator shown in Figure 1(c). The corresponding actuator input $\mathbf{d}_1$ is calculated from

$$\mathbf{d}_1=\sqrt{\mathbf{x}_1^2+\mathbf{y}_1^2} \tag{10}$$

Similarly, for $\mathbf{r}_i=\mathbf{r}_2$, $\mathbf{x}_E=\mathbf{x}_p$, $\mathbf{y}_E=\mathbf{y}_p$, $\mathbf{m}=\mathbf{tan}\ \alpha_2$ and $\mathbf{n}=-\mathbf{r}_0\ \mathbf{tan}\ \alpha_2$, the simultaneous solution of the equations in Eq. 8 will give two intersection points $(\mathbf{x}_2, \mathbf{y}_2)_1$ and $(\mathbf{x}_2,$

Table I. Inverse position solution of the manipulators in Figure 1. The translational qualities are in "units", and rotational quantities are in "degrees".

	RRRRR	RRRRP	PRRRP	RPRPR	RRRPR	RPRRP
$\mathbf{x}_p$	15.0	5.0	5.0	5.0	5.0	4.0
$\mathbf{y}_p$	15.0	10.0	10.0	10.0	10.0	12.0
$\mathbf{r}_0$	10.0	10.0	10.0	10.0	5.0	5.0
$\mathbf{r}_1$	10.0	10.0	10.0	–	10.0	10.0
$\mathbf{r}_2$	15.0	10.0	10.0	–	10.0	–
$\mathbf{r}_3$	15.0	10.0	–	–	–	–
$\mathbf{r}_4$	10.0	–	–	–	–	–
α_1	–	–	70	–	–	–
α_2	–	–	120	–	–	–
α	–	150	–	–	–	100
$\mathbf{x}_C, \mathbf{y}_C$	$\mathbf{x}_p, \mathbf{y}_p$	$\mathbf{x}_p, \mathbf{y}_p$	–	–	$\mathbf{x}_p, \mathbf{y}_p$	–
$\mathbf{x}_D, \mathbf{y}_D$	0.0, 0.0	0.0, 0.0	–	–	0.0, 0.0	–
$\mathbf{x}_E, \mathbf{y}_E$	–	$\mathbf{x}_p, \mathbf{y}_p$	$\mathbf{x}_p, \mathbf{y}_p$	–	–	$\mathbf{x}_p, \mathbf{y}_p$
$(\mathbf{x}_1, \mathbf{y}_1)_1$	9.96196, 0.87137	9.9162, 1.2919	0.40668, 1.11735	–	9.9162, 1.2919	–
$(\mathbf{x}_1, \mathbf{y}_1)_2$	0.87137, 9.96196	–4.9162, 8.7081	7.19097, 19.757	–	–4.9162, 8.7081	–
$(\mathbf{x}_2, \mathbf{y}_2)_1$	19.9642, 0.845262	8.74178, 0.72643	9.40864, 1.02426	–	–	4.64369, 2.02074
$(\mathbf{x}_2, \mathbf{y}_2)_2$	2.53579, 6.65474	–4.90204, 8.60369	–0.5689, 18.3059	–	–	1.19176, 21.5976
$(\theta_1, \theta_2)_1$	4.9989, 4.8488	–	–	–	–	–
$(\theta_1, \theta_2)_2$	85.0011, 138.2813	–	–	–	–	–
$(\theta)_1, (\theta)_2$	– –	7.4228, 119.4471	–	–	7.4228, 119.4471	–
$(\mathbf{d})_1, (\mathbf{d})_2$	–	1.4529, 17.2074	–	–	11.1803,	–
$(\mathbf{d}_1, \mathbf{d}_2)_1$	–	–	1.1891, 1.1827	11.1803, 11.1803	–	12.6491, 5.7248
$(\mathbf{d}_1, \mathbf{d}_2)_2$	–	–	21.025, 21.1378	–	–	–, 23.3247

https://doi.org/10.1017/S0263574701003666 Published online by Cambridge University Press

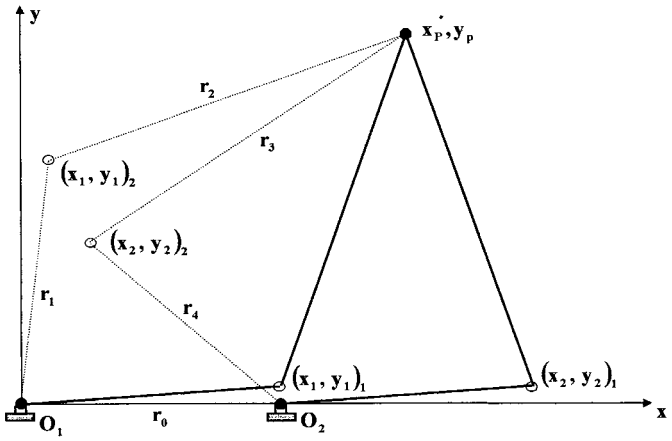


Fig. 4. Assembly configurations of inverse position solutions for RRRRR manipulator.

$\mathbf{y}_2)_2$ which are the Cartesian coordinates of the tip of the link $\mathbf{O_2B}$. The corresponding actuator input $\mathbf{d}_2$ is calculated from the vectorial equation

$$\vec{\mathbf{d}}_2 = \overrightarrow{\mathbf{O_1B}} - \overrightarrow{\mathbf{O_1O}}_2 \Rightarrow \mathbf{d}_2 = \sqrt{(\mathbf{x}_2 - \mathbf{r}_0)^2 + \mathbf{y}_2^2} \tag{11}$$

3.4 RPRPR manipulator

The inverse position solution of the RPRPR manipulator shown in Figure 1(d) is trivial. The actuator inputs $\mathbf{d}_1$ and $\mathbf{d}_2$ are found as

$$\mathbf{d}_1 = \sqrt{\mathbf{x}_p^2 + \mathbf{y}_p^2}, \quad \mathbf{d}_2 = \sqrt{(\mathbf{r}_0 - \mathbf{x}_p)^2 + \mathbf{y}_p^2} \tag{12}$$

3.5 RRRPR manipulator

For $\mathbf{r}_i = \mathbf{r}_2$, $\mathbf{r}_j = \mathbf{r}_1$, $\mathbf{x}_C = \mathbf{x}_p$, $\mathbf{y}_C = \mathbf{y}_p$ and $\mathbf{x}_D = \mathbf{y}_D = \mathbf{0.0}$, the simultaneous solution of the equations in Eq. 7 give two intersection points $(\mathbf{x}_1, \mathbf{y}_1)_1$ and $(\mathbf{x}_1, \mathbf{y}_1)_2$ which are the Cartesian coordinates of the tip of the link $\mathbf{O_1A}$ of the RRRPR manipulator shown in Figure 1(e). By using **atan2** function, the joint input θ is determined. The actuator input **d** is evaluated from

$$\mathbf{d} = \sqrt{(\mathbf{r}_0 - \mathbf{x}_p)^2 + \mathbf{y}_p^2} \tag{13}$$

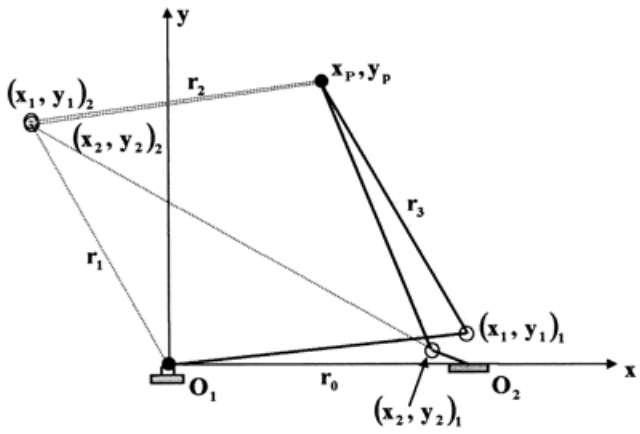


Fig. 5. Assembly configurations of inverse position solutions for RRRRP manipulator.

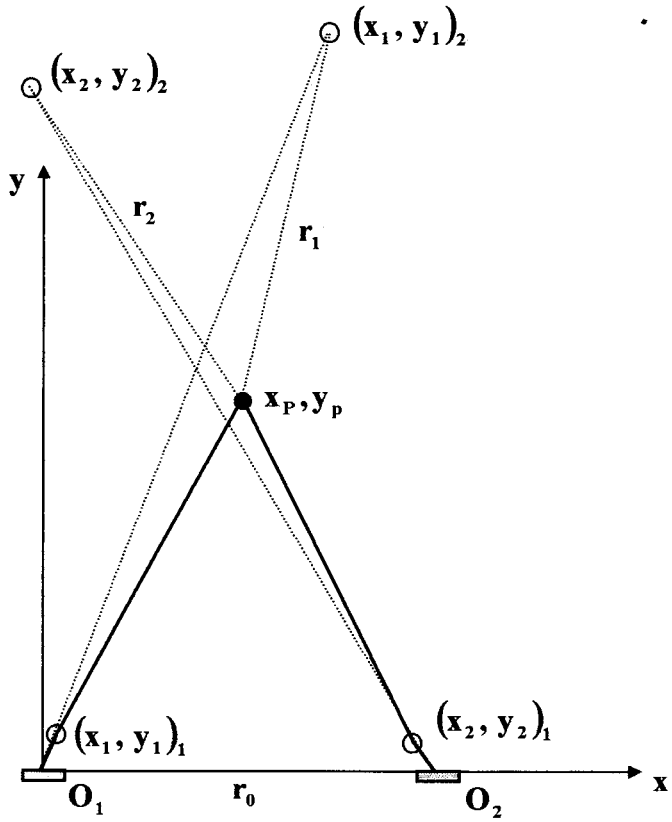


Fig. 6. Assembly configurations of inverse position solutions for PRRRP manipulator.

3.6 RPRRP Manipulator

The actuator input **d** is simply determined from

$$\mathbf{d}_1 = \sqrt{\mathbf{x}_p^2 + \mathbf{y}_p^2} \tag{14}$$

For $\mathbf{r}_i = \mathbf{r}_1$, $\mathbf{x}_E = \mathbf{x}_p$, $\mathbf{y}_E = \mathbf{y}_p$, $\mathbf{m} = \mathbf{tan}\ \alpha$ and $\mathbf{n} = -\mathbf{r}_0\ \mathbf{tan}\ \alpha$, the simultaneous solution of the equations in Eq. 8 will give two intersection points $(\mathbf{x}_2, \mathbf{y}_2)_1$ and $(\mathbf{x}_2, \mathbf{y}_2)_2$ which are the Cartesian coordinates of the tip of the link $\mathbf{O_2B}$. The

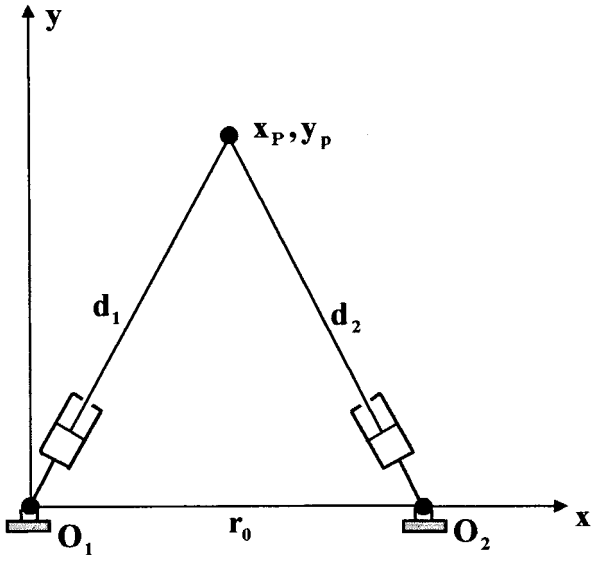


Fig. 7. Assembly configuration of inverse position solutions for RPRPR manipulator.

https://doi.org/10.1017/S0263574701003666 Published online by Cambridge University Press

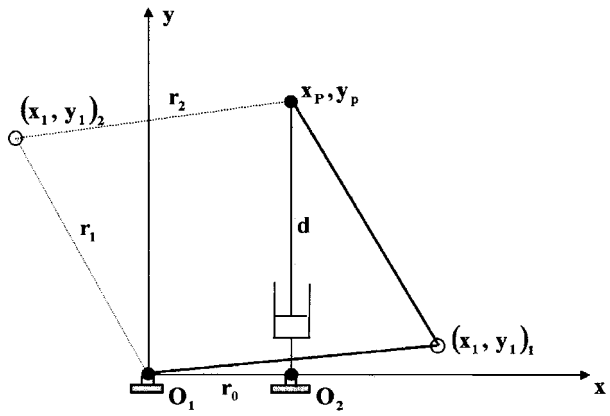


Fig. 8. Assembly configurations of inverse position solutions for RRRPR manipulator. Note that the actuator length **d** does not change for both configurations.

corresponding actuator input $\mathbf{d}_2$ is calculated from the vectorial equation

$$\vec{\mathbf{d}}_2 = \overrightarrow{\mathbf{O}_1\mathbf{B}} - \overrightarrow{\mathbf{O}_1\mathbf{O}}_2 \Rightarrow \mathbf{d}_2 = \sqrt{(\mathbf{x}_2 - \mathbf{r}_0)^2 + \mathbf{y}_2^2} \qquad (15)$$

4. SYLVESTER ELIMINATION METHOD

It is a direct method to obtain all solutions of **n** nonlinear polynomial equations. It is not an iteration method, but of an elimination method to find all possible solutions. It is based on an algebraic formulation that makes possible to eliminate a large number of variables and hence reduces a set of nonlinear equations to a single variable polynomial whose roots are a set of solutions. A full account of this method is given in reference [16]. For the problem at hand, there exist two nonlinear polynomial equations $\mathbf{p}^{th}$ degree and $\mathbf{q}^{th}$ degree, respectively, in two unknowns, say **x** and **y**. The procedure for Sylvester elimination method applied to a binary system is given below;

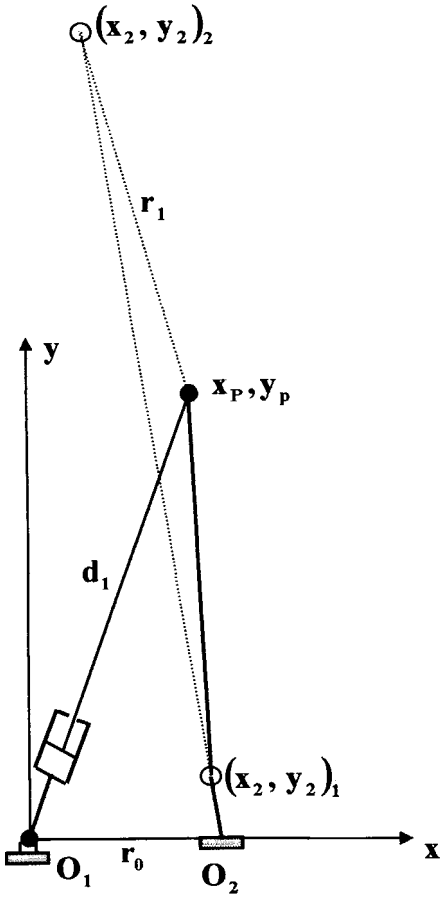


Fig. 9. Assembly configurations of inverse position solutions for RPRRP manipulator. Note that the actuator length $\mathbf{d}_1$ does not change for both configurations.

(i) Rewrite the two equations in the form of descending power of one of the unknowns so that that unknown can be eliminated, as given below;

$$\begin{aligned} \mathbf{a}_p\mathbf{x}^p + \mathbf{a}_{p-1}\mathbf{x}^{p-1} + \mathbf{a}_{p-2}\mathbf{x}^{p-2} + \cdots + \mathbf{a}_0 = \mathbf{0} \\ \mathbf{b}_q\mathbf{x}^q + \mathbf{a}_{q-1}\mathbf{x}^{q-1} + \mathbf{a}_{q-2}\mathbf{x}^{q-2} + \cdots + \mathbf{b}_0 = \mathbf{0} \end{aligned} \qquad (16)$$

Note the coefficients $\mathbf{a}_i$ and $\mathbf{b}_i$ are functions of the other unknown **y**.

(ii) Multiply the first equation and the second equation successively by **x**, $\mathbf{q}-1$ times and $\mathbf{p}-1$ times, respectively;

$$\begin{aligned} &\mathbf{a}_p\mathbf{x}^{p+1} + \mathbf{a}_{p-1}\mathbf{x}^p + \mathbf{a}_{p-2}\mathbf{x}^{p-1} + \cdots + \mathbf{a}_0\mathbf{x} = \mathbf{0} \\ &\mathbf{a}_p\mathbf{x}^{p+2} + \mathbf{a}_{p-1}\mathbf{x}^{p+1} + \mathbf{a}_{p-2}\mathbf{x}^{p-1} + \cdots + \mathbf{a}_0\mathbf{x}^2 = \mathbf{0} \\ &\vdots \\ &\mathbf{a}_p\mathbf{x}^{p+q-1} + \mathbf{a}_{p-1}\mathbf{x}^{p+q-2} + \mathbf{a}_{p-2}\mathbf{x}^{p+q-3} + \cdots + \mathbf{a}_0\mathbf{x}^{p-1} = \mathbf{0} \\ &\mathbf{b}_q\mathbf{x}^{q+1} + \mathbf{a}_{q-1}\mathbf{x}^q + \mathbf{a}_{q-2}\mathbf{x}^{q-1} + \cdots + \mathbf{b}_0\mathbf{x} = \mathbf{0} \\ &\mathbf{b}_q\mathbf{x}^{q+2} + \mathbf{a}_{q-1}\mathbf{x}^{q+1} + \mathbf{a}_{q-2}\mathbf{x}^{q-1} + \cdots + \mathbf{b}_0\mathbf{x}^2 = \mathbf{0} \\ &\vdots \\ &\mathbf{b}_q\mathbf{x}^{q+p-1} + \mathbf{a}_{q-1}\mathbf{x}^{q+p-2} + \mathbf{a}_{q-2}\mathbf{x}^{q+p-3} + \cdots + \mathbf{b}_0\mathbf{x}^{p-1} = \mathbf{0} \end{aligned} \qquad (17)$$

The $(\mathbf{p}+\mathbf{q})$ equations given in Eq. 17 are rewritten in the matrix-vector form as;

$$\mathbf{E}\boldsymbol{\varepsilon} = \mathbf{0} \qquad (18)$$

where **E** is the $(\mathbf{p}+\mathbf{q})$ **x** $(\mathbf{p}+\mathbf{q})$ coefficient matrix of the $\mathbf{p}+\mathbf{q}$ augmented equations in Eq. 17, $\boldsymbol{\varepsilon}$ is the vector containing the unknown **x** and its powers. The equation 18 can be satisfied if and only if the determinant of the coefficient matrix **E**, which is called the eliminant of the set of equations considered, is zero. The degree of the resulting polynomial indicates the number of common solutions. The roots of the eliminant are common root(s) of the equations. The calculated roots are substituted into the equation set such that two equations with one unknown but with numerical coefficients is obtained. In order to evaluate the common roots corresponding to the roots calculated from the eliminant, the "Remainder Polynomial" of the the $\mathbf{p}^{th}$ degree and $\mathbf{q}^{th}$ degree polynomials is found. The roots of the remainder polynomial gives the set of all solutions.

This procedure now can be employed to solve the equations in Eq. 7, the first equation in Eq. 7 is multiplied by **x** and hence, an extra equation is obtained. Also, the second equation in Eq. 7 is multiplied by **x** and another extra equation is obtained. Thus, the following augmented set of four equations came into existence;

$$\begin{aligned} &\mathbf{x}^2 - (2\mathbf{x}_C)\mathbf{x} + (-\mathbf{r}_i^2 + \mathbf{x}_C^2 + \mathbf{y}^2 - 2\mathbf{y}\mathbf{y}_C + \mathbf{y}_C^2) = \mathbf{0} \\ &\mathbf{x}^3 - (2\mathbf{x}_C)\mathbf{x}^2 + (-\mathbf{r}_i^2 + \mathbf{x}_C^2 + \mathbf{y}^2 - 2\mathbf{y}\mathbf{y}_C + \mathbf{y}_C^2)\mathbf{x} = \mathbf{0} \\ &\mathbf{x}^2 - (2\mathbf{x}_D)\mathbf{x} + (-\mathbf{r}_j^2 + \mathbf{x}_D^2 + \mathbf{y}^2 - 2\mathbf{y}\mathbf{y}_D + \mathbf{y}_D^2) = \mathbf{0} \\ &\mathbf{x}^3 - (2\mathbf{x}_D)\mathbf{x}^2 + (-\mathbf{r}_j^2 + \mathbf{x}_D^2 + \mathbf{y}^2 - 2\mathbf{y}\mathbf{y}_D + \mathbf{y}_D^2)\mathbf{x} = \mathbf{0} \end{aligned} \qquad (19)$$

https://doi.org/10.1017/S0263574701003666 Published online by Cambridge University Press

This set of equations can be rewritten in the matrix-vector form;

$$\begin{bmatrix} \mathbf{0} & \mathbf{1} & -2\mathbf{x}_C & -\mathbf{r}_i^2+\mathbf{x}_C^2+\mathbf{y}^2-2\mathbf{y}\mathbf{y}_C+\mathbf{y}_C^2 \\ \mathbf{1} & -2\mathbf{x}_C & -\mathbf{r}_i^2+\mathbf{x}_C^2+\mathbf{y}^2-2\mathbf{y}\mathbf{y}_C+\mathbf{y}_C^2 & \mathbf{0} \\ \mathbf{0} & \mathbf{1} & -2\mathbf{x}_D & -\mathbf{r}_j^2+\mathbf{x}_D^2+\mathbf{y}^2-2\mathbf{y}\mathbf{y}_D+\mathbf{y}_D^2 \\ \mathbf{1} & -2\mathbf{x}_D & -\mathbf{r}_j^2+\mathbf{x}_D^2+\mathbf{y}^2-2\mathbf{y}\mathbf{y}_D+\mathbf{y}_D^2 & \mathbf{0} \end{bmatrix} \begin{bmatrix} \mathbf{x}^3 \\ \mathbf{x}^2 \\ \mathbf{x} \\ \mathbf{1} \end{bmatrix} = \begin{bmatrix} \mathbf{0} \\ \mathbf{0} \\ \mathbf{0} \\ \mathbf{0} \end{bmatrix} \quad (20)$$

The solutions for the set of equations in Eq. 7 exist if and only if the determinant of the coefficient matrix of Eq. 20, which is the eliminant of the equations, is equal to zero. For the case under study, the resulting eliminant is a second order nonlinear polynomial in **y**. This follows that the number of solutions is two. Each root of the eliminant is substituted into the two equations. Note that the equations now have numerical coefficients. The roots of the remainder polynomial of the two equations give the common solutions for the two equations. These solutions $(\mathbf{x}, \mathbf{y})_1$ and $(\mathbf{x}, \mathbf{y})_2$ are the Cartesian coordinates of intersection points of the two circles, as shown in Figure 3(a).

The same procedure is applied to Eq. 8 to compute the Cartesian coordinates of intersection points of a circle a with a line. The first equation in Eq. 8 is left as it is, but the second in Eq. 8 is multiplied by **x** and an extra equation is obtained. The matrix-vector form of these augmented set of equations is;

$$\begin{bmatrix} \mathbf{1} & -2\mathbf{x}_E & -\mathbf{r}_i^2+\mathbf{x}_E^2+\mathbf{y}^2-2\mathbf{y}\mathbf{y}_E+\mathbf{y}_E^2 \\ \mathbf{0} & \mathbf{m} & -\mathbf{y}-\mathbf{n} \\ \mathbf{m} & -\mathbf{y}-\mathbf{n} & \mathbf{0} \end{bmatrix} \begin{bmatrix} \mathbf{x}^2 \\ \mathbf{x} \\ \mathbf{1} \end{bmatrix} = \begin{bmatrix} \mathbf{0} \\ \mathbf{0} \\ \mathbf{0} \end{bmatrix} \quad (21)$$

Note that the coefficient matrix of Eq. 21 is a 3×3 matrix and its determinant is a second order nonlinear polynomial in **y**. This follows that the number of solutions is two. Each root of the eliminant is substituted into the two equations. The roots of the remainder polynomial of the two equations give the common solutions for the two equations. These solutions $(\mathbf{x}, \mathbf{y})_1$ and $(\mathbf{x}, \mathbf{y})_2$ are the Cartesian coordinates of intersection points of a circle with a line, as shown in Figure 3(b).

5. NUMERICAL RESULTS

For provided link lengths $\mathbf{r}_i$, the Cartesian coordinates ($\mathbf{x}_p$, $\mathbf{y}_p$) of the manipulator tip point **P** and those of the actuators (active joints), the equations given through Section 3.1 to 3.6 are solved by employing the elimination method presented in the previous section. All the solutions for the manipulators depicted in Figure 1 are tabulated in Table I. The assembly configurations of the manipulators are shown in Figures 4 to 9. The solutions are verified by substituting them into the forward kinematics given by Eq. 5 and Eq. 6.

6. CONCLUSIONS

We have presented a simple and efficient method to determine inverse position of a class of five-bar planar parallel manipulators. Numerical examples are provided to demonstrate the method. This study contributes to previously published work from the point of view of being simple and systematic, and requiring small computation time.

References

1. G. Alici, "Determination of Singularity Contours for Five-bar Planar Parallel Manipulators", *Robotica* **18**(6), 569–575 (2000).
2. H. Ovayolu and G. Alici, "Closed-form Forward Kinematics Analysis of a 6–3 Parallel Manipulator." *13th International Conference On CAD/CAM Robotics and Factories of the Future*, Pereira, Colombia (December, 1997), pp. 232–240.
3. F.H. Ghorbel, O. Chetelat, R. Gunawardana and R. Longchamp, "Modelling and Set Point Control of Closed-Chain Mechanisms: Theory and Experiments", *IEEE Transactions on Control Systems Technology* **8**(5), 801–815 (September, 2000).
4. A.A. Goldenberg, B. Benhabib and R.G. Fenton, "A Complete Generalised Solution to the Inverse Kinematics of Robots", *IEEE J. of Robotics and Automation* **RA-1**(1), 14–28 (January, 1985).
5. V.D. Tourassis and M.H. Ang Jr. "A Modular Architecture for Inverse Robot Kinematics", *IEEE Trans. of Robotics and Automation* **5**(5), 555–568 (October, 1989).
6. J. Nielsen and B. Roth, "On the Kinematic Analysis of Robotic Mechanisms", *Int. J. Robotics Research* **18**(12), 1147–1160 (December, 1999).
7. C. Wampler and Alexander Morgan, "Solving the 6R Inverse Position Problem Using a Generic-Case Solution Methodology", *Mechanism and Machines Theory* **26**(1), 91–106 (1991).
8. D. Manocha and J.F. Canny, "Efficient Inverse Kinematics for General 6R Manipulators", *IEEE Transactions on Robotics and Automation* **10**(5), 648–657 (October, 1994).
9. H.Y. Lee and C.G. Liang, "Displacement Analysis of The Spatial 7-Link 6R-P Linkages", *Mechanism and Machines Theory* **22**(1), 1–11 (1987).
10. M. Raghavan and B. Roth, "Kinematic Analysis of the 6R Manipulator of General Geometry", *Fifth International Symposium on Robotics Research*, Tokyo (1989) pp. 314–320.
11. C. Innocenti and V. Parenti-Castelli, "Closed-Form Direct Position Analysis of A 5–5 Parallel Mechanism", *ASME J. of Mechanical Design* **115**, 515–521 (1993).
12. H. Zhang and R.P. Paul, "A parallel kinematics solution for robot manipulators based on multiprocessing and linear extrapolation", *IEEE Transactions on Robotics and Automation* **7**(5), 660–669 (October, 1991).
13. S. Elgazzar, "Efficient Kinematic Transformations for the PUMA 560 Robot", *IEEE J. of Robotics and Automation* **RA-1**(3), 142–151 (September, 1985).
14. J.J. Cervantes-Sanchez and J. G. Rendon-Sanchez, "A simplified approach for obtaining the workspace of a class of 2-dof planar parallel manipulators", *Mechanism and Machines Theory* **34**, 1057–1073 (1999).
15. Y. Nakamura, *Advanced Robotics: Redundancy and Optimization* (Addison-Wesley Publishing Company, 1991).
16. J.J. Sylvester, *The Collected Mathematical Papers of James Joseph Sylvester* (Chelsea Publishing Company, New York, 1973), **Vol. 1**.

https://doi.org/10.1017/S0263574701003666 Published online by Cambridge University Press